Poly(propylene imine) dendrimers can bind to PEGylated albumin at PEG and albumin surface. Biophysical examination of a PEGylated platform to transport cationic dendritic nanoparticles.

Karol Ciepluch, Ralf Biehl, Maria Bryszewska and Michał Arabski*

Dr. K. Ciepluch, Dr. M. Arabski
Department of Medical Biology, Jan Kochanowski University, Kielce, Poland
E-mail: karol.ciepluch@ujk.edu.pl

Dr. R. Biehl
Jülich Centre for Neutron Science & Institute of Complex Systems (JCNS-1&ICS-1), Forschungszentrum Jülich, Germany.

Prof. M. Bryszewska
Department of General Biophysics, University of Lodz, Poland.

Keywords: PEGylation, albumin platform, PPI dendrimers, drug development

Abstract
Cationic dendrimers are considered one of the best drug transporters in the body. However, in order to improve their biocompatibility, modification of them is required to reduce toxicity. In this way many dendrimers may lose their original properties, e.g. anti-cancer. To improve biocompatibility of dendrimers, it is possible to complexation them with albumin as is very often in drug delivery. However, the interaction of dendrimers with albumin lead to protein structure disruption or not complexation at all. Therefore, investigation the interaction between cationic poly-(propylene imine) dendrimers and PEG-albumin by fluorescence, circular dichroism, small angle X-ray scattering SAXS, transmission electron microscope were done. Results have shown that cationic dendrimers bind to PEGylated albumin at PEG and albumin surfaces. The obtained results for 5k-PEG indicates a preferential binding of the dendrimers to PEG. For 20k-PEG binding of dendrimers to PEG and protein could induce a collapse of the PEG chain onto the protein surface. This opens up new possibilities to the use of PEGylated albumin as a platform to carry dendrimers without changes the albumin structure and improve the pharmacokinetic properties of dendrimers without further modification.

1. Introduction

Dendrimers are now seen as one of the most promising tools in the field of nanobiotechnology [1]. They show great potential in gene therapy, drug delivery, medical imaging and as antimicrobial and antiviral agent [2,3]. Dendrimers are monodisperse, multi-functionalized and hyperbranched polymers of nanometers in size. The structural features and the high density of their chemical reactive sites on the outer shell enhances their use in biology and medicine [4].
Dendrimers are used as a drug carrier, but have they also have anticancer and antimicrobial potential [5,6]. The main problem of cationic dendrimers is toxicity due to their surface charge [7,8]. However, the excess of cationic surface group helps them to overcome membrane barriers [9] and promotes their use as an anticancer agent, but on the negative side they can be toxic to

normal healthy cells and cause other side effects. The modification of a dendrimer surface, e.g. with polyethylene glycol or sugar, leads to a decrease in toxicity [10–12].
Due to their cationic surface, dendrimers tend to aggregate and cannot be easily transported through the circulatory blood system because of their activation of the immune system. If they are considered as drugs or drug carrier, they have to be protected by something that makes them non-toxic and non-immunogenic, for instance albumins. There are many reports of the interactions between dendrimers and albumin, both bovine serum albumin (BSA) and human serum albumin (HSA) [13–15].
Nowadays, researchers are trying hard to develop advanced, effective and, at the same time, secure drug delivery systems. The therapeutic efficiency of a drug is dependent on the availability of the target site and drug concentration, which both need to be effective and non-toxic. Therapeutic drugs are very often low-molecular weight molecules with rapid renal clearance and short plasma circulatory times. On the other side, many therapeutic drugs, e.g., nanoparticles or synthetic polymers, tend to aggregate and accumulate in human organs [16]. Therefore, drug delivery technology requires new methods to overcome these barriers. The perfect candidate to achieve these goals could be albumin. Albumin is not a drug itself, but it can be considered as a carrier for transporting drugs in the blood, i.e. of exogenous as well as endogenous compounds, it seems quite natural to use albumin to improve drug delivery of pharmaceutics [17,18]. Albumin is the most abundant plasma protein with a molecular weight of 66.5 kDa, comprising 584 amino acids with strong negative charge. In recent years, albumin has emerged as a versatile carrier for therapeutic and diagnostic agents, primarily for diagnosing and treating diabetes, cancer and infectious diseases[19]. Several drugs are based on albumin, e.g. taxol albumin nanoparticle Abraxane for treating metastatic breast cancer [20,21]. The conjugation of albumin with other nanoparticles and therapeutic drugs enhance distribution and bioavailability of these molecules [22–24]. Currently, albumin is considered as a best carrier for many anticancer drug-nanoparticles, which normally can cause serious damage of the surrounding healthy cells. Modification with albumin brings many benefits, [25,26] e.g. its complexes tend to accumulate in solid tumors [17].
In association with albumin, dendrimers may change the albumin structure or due to high molecular mass they cannot be attached to albumin surface and be transported in blood. Therefore, we tested whether it is possible to complexing dendrimers with albumin by the latter being modified by polyethylene glycol (PEG). PEGylation of proteins is used to improve bio-compatibility of drug proteins and decrease immunogenicity [27]. We have combined dendrimers with PEG-Albumin through electrostatic interactions to use the protective character of.
The main aim has been to examine the effect of PEG length on interactions between cationic dendrimers and albumin, specifically BSA. The nature of the PEG in albumin-dendrimer complex may be important when we consider using PEGylated albumin as a platform to carry dendrimers. Polypropylene imine dendrimers (in the following dendrimers, see **Figure 1**) were chosen as a polycationic dendrimer model.

2. Experimental section

2.1. Materials

Methoxypolyethylene glycol maleimide-PEG 5,000 was purchased from Sigma Aldrich, and methoxypolyethylene glycol maleimide-PEG 20,000 was purchased from creative PEGWork. BSA and other chemicals were of analytical grade. Fourth generation (G4) poly(propylene imine) dendrimer with a diamino-butane core and peripheral primary amine groups was obtained from SyMo-Chem (Eindhoven, The Netherlands).

2.2 PEGylation of BSA

About 1.5 mol of solid mPEG-maleimide reagent was added per mol of protein to 5 ml 20 mg/mL BSA and the solution mixed at room temperature overnight. All solutions were made in 10 mmol/L phosphate-buffered saline (PBS) at pH 7.4. To stop reactions, samples were acidified with one drop of 0.1 mol/L HCl. The samples were separated using size exclusion chromatography (SEC) BioGel (Bio-Rad) Column with PBS. The column was equilibrated with 1 CV of 10 mmol/L PBS pH 7.4 and samples were eluted (1 CV) with flow rate of 1 ml/min. All purification was carried out using Bio-Rad chromatography system (Bio-Rad, USA). PEGylated proteins were monitored, collected and detected by SDS PAGE. In the following experiments, we used 5and 20k Da maleimide PEGs.

2.3 Protein-dendrimer complex formation

In each experiment dendrimers were directly added to the protein solution in a molar ratio of 1:4 and were analyzed without further purification.

2.4 Fluorescence quenching of BSA and PEG-BSA

BSA, 5k-PEG-BSA and 20k-PEG-BSA were dissolved in PBS at 10 μmol/L. The excitation wavelength of 290 nm was used and the emission spectra were recorded at 340 nm, using slit widths of 10 nm. Next, dendrimers were added (up to 1:4 molar ratio) and fluorescence spectra were recorded.

2.5 Circular dichroism (CD) measurements

The CD spectra were measured with a Spectrometer Jasco J-815 (Japan). The cuvette with a 1 cm path length, and 10 mmol/L PBS pH 7.2 as a running buffer were used. BSA, 5k-PEG-BSA and 20k-PEG-BSA were dissolved at 0.1 mmol/L. Molar ratio of dendrimer/protein ranged from 1 to 8. The spectrometer was continuously purged with dry nitrogen before and during the experiment. The spectra were recorded from 200 to 260 nm. All spectral data were presented as a mean residue ellipticity or molar ellipticity (θ).

2.6 Small Angle X-ray Scattering (SAXS) analysis

SAXS experiments used a SAXSpace (Anton Paar) at Forschungszentrum Jülich at a wavelength of λ=0.154 nm, and the covering scattering vectors Q from 0.1 to 6 nm ($Q=4\pi\sin(\theta/2)/\lambda$, where θ is the scattering angle). SAXS data were treated and radially averaged by the respective instrument software. Empty cells and buffer values were subtracted as background and finally normalized for BSA concentrations. The coherent scattering intensity of particles in solution with background contributions bgr is given by the equation:

$$I(Q) = (N/V)S(Q)F(Q) + bgr \qquad (1)$$

with the number of particles N in the volume V. The interparticle interactions are subsumed in the structure factor S(Q). The data were extrapolated to zero concentration to extract the BSA form factor. BSA solutions with and without dendrimers in PBS at pH 7.4 were measured for their protein concentration in the range from 5 to 30 mg/ml at 20°C. The BSA: dendrimer molar ratio was always 1:4. The radius of gyration (Rg) describes the size of protein-dendrimer complex.

2.7 Microfluidics-based electrophoresis

Microfluidics-based electrophoresis (SDS-PAGE, non-reducing conditions) used an Agilent 2100 Bioanalyzer with the Sensitive Protein 250 Lab Chip Kit, supplied by Agilent Technologies, Waldbronn, Germany. BSA samples where labelled with fluorescent dye (part of the Sensitive Protein 250 Lab Chip Kit, Agilent). After loading the gel-dye mix into the chip using the chip-priming station, labeled samples and ladder were pipetted in the corresponding wells on the chip. Finally, it was inserted in the Bioanalyzer and the run began. The data were analyzed by Bioanalyzer 2100 Expert Software.

2.8 Transmission electron microscopy

The morphology of complexes of polypropylene imine dendrimers with BSA/PEG-BSA was examined by TEM (JEOL-10, JEOL Ltd., Tokyo, Japan). The dendrimers were added to BSA at a molar ratio of 1:4 (dendrimer to BSA). The complexes were placed on the carbon surface of 200-mesh copper grid (Ted Pella, Inc., USA) for 10 min and drained with blotting paper. Samples were negatively stained with 2% (w/v) uranyl acetate for 2 min, and viewed at a magnification of 60,000x.

3. Results and discussion

3.1 Interactions between dendrimers and proteins.

A well-established method to examine the interactions of nanoparticles with proteins is fluorescence quenching of tryptophan (Trp). BSA contains 2 Trp residues, one being located on the protein surface (Trp134) and the other being buried inside of the protein (Trp213). The intrinsic protein fluorescence gives us information about the local environment around the Trp as specific interactions with the solvent or attached molecules change the fluorescent output. A change of the local environment to be more hydrophobic or hydrophilic increases or decreases, respectively, the fluorescence; an increase in pH increases the quantum yield as static quenching[28]. Dynamic quenching due to collisions with solvent molecules reduces fluorescence intensity. For HSA and BSA, 5 possible binding "sites" of cationic dendrimers were found [29]. In these sites, aspartic and glutamic acid form local regions with negative charge (Figure 1). The possible sites are located on domain IB (3 sites) and domain IIB (2 sites). Trp is localized in domain IB, making Trp fluorescence very sensitive to changes on the surface of the IB domain. The mixing ratio between dendrimers and BSA was 4:1 molar. The fluorescence intensity at 340 nm of BSA and PEG-BSA in PBS solution with dendrimers are shown in Figure 2. PEGylation increases the fluorescence intensity to 110% for 5k-PEG and 120% for 20k-PEG.

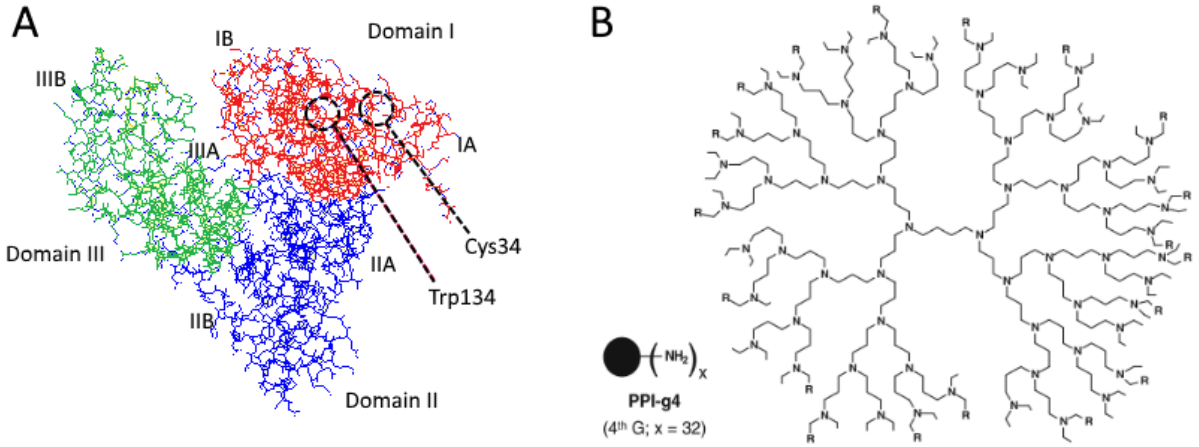

Figure 1. *Structure of bovine serum albumin with three different domains. Cys34 (place where PEG is attached) and Trp134 are localized on the same domain (A). The chemical structure of polypropylene(imine) dendrimers with amine terminated groups on the surface and a molecular weight of about 3600 Da (B). G4 PPI dendrimers have a Rg of about 1.2 nm and geometrical radius of about 1.3 nm [30,31].*

The changes are due to the ambivalent character of PEG showing both its hydrophilic to amphiphilic tendencies dependent on molecular weight and binding environment [32,33]. In the present case, PEG seems to present a more hydrophobic environment to Trp, leading to a slight increase in intensity, which might be due to PEG not binding to the surface, but to its wrapping around the protein in a more extended configuration. However, addition of dendrimer leads to 3 different changes in fluorescence. Trp quenching in the presence of dendrimers alone was decreased by 30%. There was only a small quenching of Trp fluorescence with 5kPEG-BSA

when dendrimers were added. The quenching with 20kPEG-BSA was the highest, at ~60% compared to the non-treated PEGylated protein. The strong Trp fluorescence quenching is very characteristic for almost all dendrimers-BSA interactions [34,35]. Collisional quenching may be due to interaction between species, where the greater the collision the more there is a decrease in fluorescence intensity. However, the dendrimers of generation 4 are quite large with a diameter ~2.6 nm, and negatively charged binding sites are small compared to the dendrimer size. The internal flexibility in dendrimer structure may lead to coverage of a large surface, including the Trp134 neighborhood that causes static quenching. The PEG attachment to the domain IB also is involved in dendrimer-protein interactions. The presence of the PEG chain should result in additional steric hindrance for the attachment of dendrimers to BSA, thereby limiting the interaction with the IB domain. For 5k-PEG, the intensity decreasing effect of the dendrimers seems to be fully compensated. For 20k-PEG-BSA, unexpectedly there was an even stronger decrease of fluorescence intensity. The value of ~60% suggests nearly full quenching of the Trp134 fluorescence contribution, the remaining intensity being mainly due to the Trp213 buried inside BSA. PEGylation here seems to strengthen the effect of adding dendrimer. As discussed later, the dendrimer might enhance the hydrophilic/amphiphilic properties of PEG, leading to an even more hydrophilic environment to Trp.

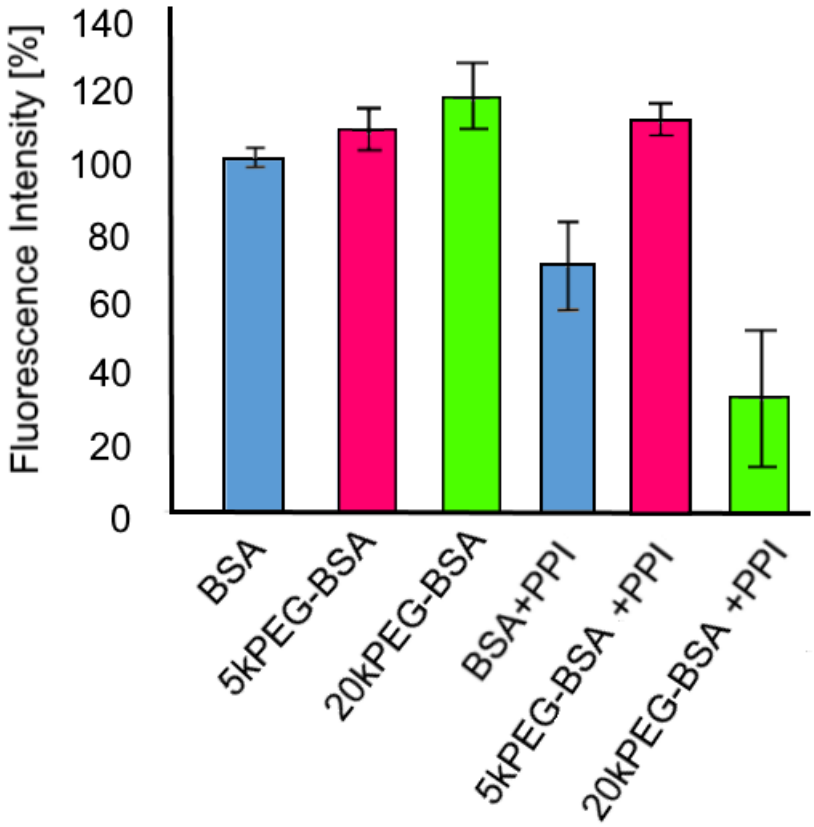

Figure 2. *BSA, 5kPEG-BSA and 20kPEG-BSA tryptophan residue fluorescence quenching by poly(propylene imine) dendrimers. The molar ratio of proteins : dendrimers was 1:4. Values are given relative to BSA taken as 100%.*

3.2 Secondary structure changes of protein due to interactions with dendrimers

To observe whether the change in fluorescence is correlated to a change in the local secondary structure around the Trp residues, CD measurements were taken. It is known that PEG

attachment neither changes the secondary structure of proteins nor the domain structure of hinge proteins [36,37]. In these measurements, the BSA, 5k-PEG-BSA and 20k-PEG-BSA were mixed with dendrimers to measure the respective changes in secondary structure of BSA (Figure 3). Only small changes due to either PEGylation or titration with dendrimers were found, and we conclude that the changes are not significant.

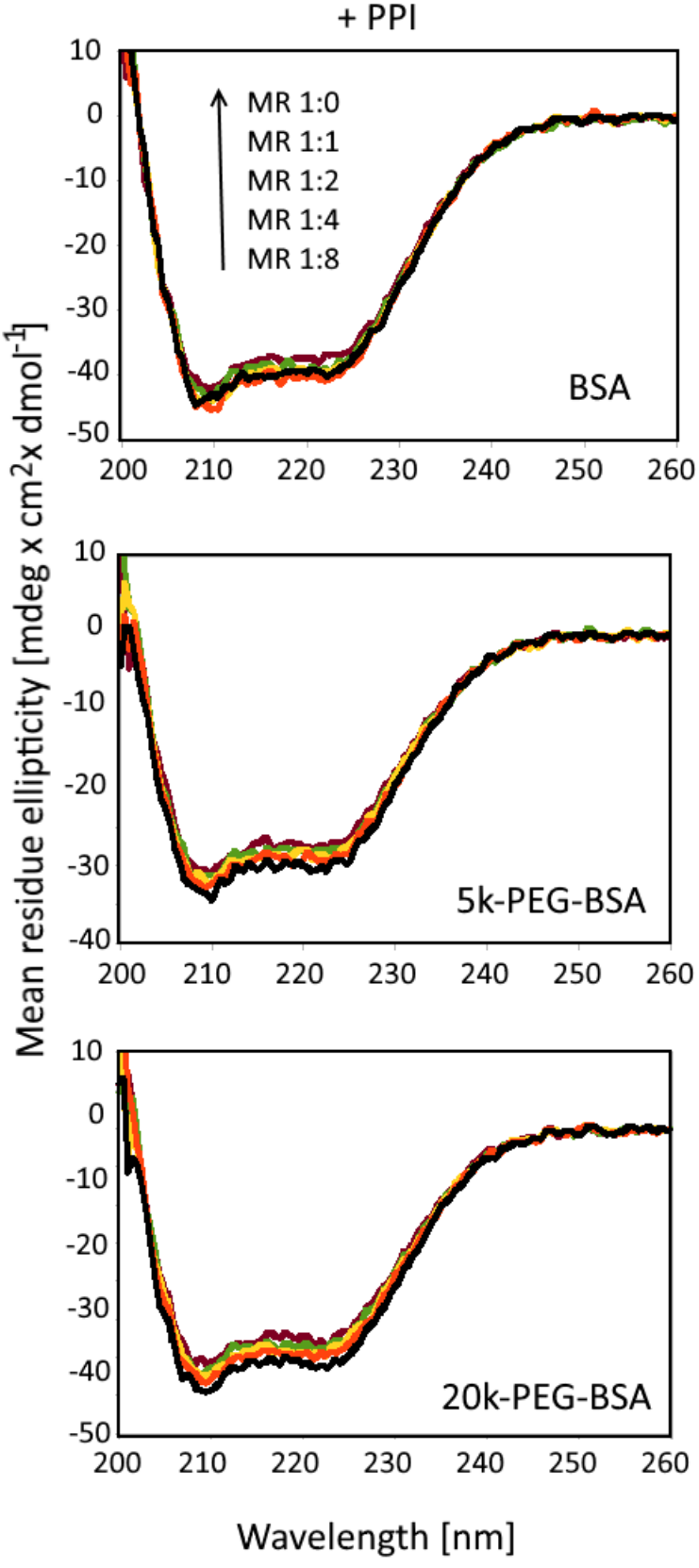

Figure 3. *CD spectra of BSA, 5k-PEG-BSA and 20k-PEG-BSA mixed with poly(propylene imine) dendrimers – PPI.*

3.3 Shape and size of PEGylated albumin complexed with dendrimers.

Dendrimer molecules attached to BSA can be observed by small angle scattering as a characteristic change in the scattering pattern. Figure 4 shows SAXS form factors as extracted from measurements of a concentration series for BSA and PEGylated BSA without and with dendrimers at a molar ratio 1:4. There was no significant contribution in SAXS shape in Q range >1.2 nm^{-1} for all samples that were tested. Small deviations at the highest Q might be due to incomplete background subtraction. The results suggest there were no protein structural changes due to PEGylation or addition of dendrimers in accordance to the CD results. The only visible changes were seen at low Q in a range between 0.2 and 1.2 nm-1. In the Guinier region (up to 0.5 nm^{-1}) there are changes in the forward scattering intensity I_0 and the radius of gyration Rg as a measure of complex size (Table 1). PEGylation increases forward scattering intensity I_0 only slightly whereas adding dendrimers makes I_0 much stronger. The increase in I_0 for all complexes with dendrimers indicates a clear binding of dendrimers; free dendrimers under the present conditions make no significant contribution. In general, the forward scattering I_0 of a compound particle depends on the displaced solvent volume V_i and the average contrast relative to the solvent ρ_i of each compound i as $I_0=(\Sigma V_i\rho_i)^2$. In first-order, by neglecting additional interactions one would expect a similar increase in $\Sigma V_i\rho_i$ for addition of dendrimers in all samples if they bind only to the protein surface without altering BSA or PEG conformation, which would otherwise lead to a change in the displaced volume. An increase in $\Sigma V_i\rho_i$ of 0.0068, 0.0125 and 0.025 for dendrimer addition to BSA, 5k-PEG-BSA and 20k-PEG-BSA was recorded, which indicates that, as well as the dendrimer contribution $V_d\rho_d$, the displaced volume of PEG or dendrimers seems to change due to a more complex interaction between charged dendrimers and PEG, assuming that the dominating the protein contribution is not changed. A detailed modelling considering the water structure around the protein, PEG and dendrimers has not been possible.

Table 1. Forward scattering intensity I0 and Radius of gyration Rg with dendrimers and without.

	I_0 (a.u.)	**Radius of gyration R*g* (nm)**
BSA	0.0400	2.77 ± 0.06
BSA + PPI Dendrimers	0.0428	2.88 ± 0.08
5k PEG-BSA	0.0407	3.00 ± 0.05
5k PEG-BSA + PPI Dendrimers	0.0459	3.20 ± 0.08
20k PEG-BSA	0.044	3.19 ± 0.11
20k PEG-BSA + PPI Dendrimers	0.0552	3.49 ± 0.05

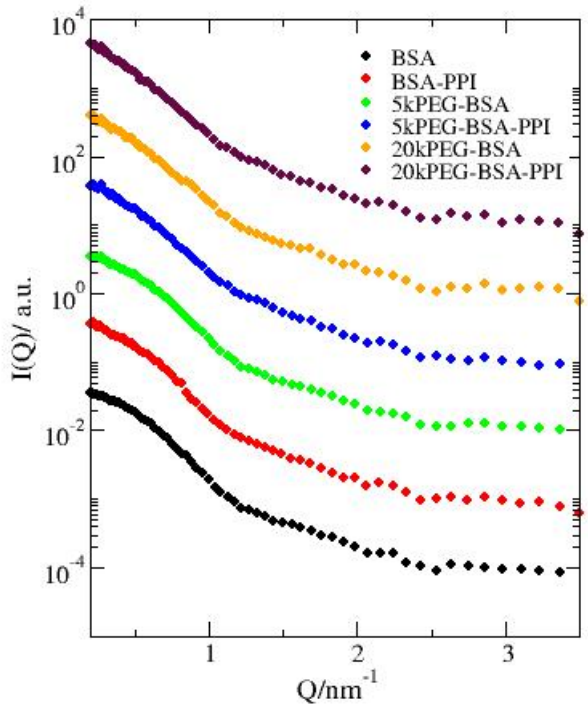

Figure 4. *SAXS form factors as extracted from concentration series measurements for BSA, 5k-PEG-BSA and 20PEG-BSA with and without PPI dendrimers. The BSA characteristic linear region between 1-2.5 nm-1 for all samples indicated preservation of protein structure. Changes were observed mainly between 0.2 and 1.2 nm-1 and represent a change in the radius of gyration due to dendrimers and PEG. Data are scaled by a factor of 10 for better visibility.*

The radius of gyration of PEGylated BSA increases the lengths of PEG and their configuration around the protein. The R_g of BSA is 2.77 nm, which increases to 3.0 nm in the case of 5 kDa PEG, and 3.19 nm with 20 kDa PEG. Addition of dendrimers results in a clear increase in R_g for all samples, with t smallest being for unPEGylated BSA, in correspondence to the smallest increase in I_0. Considering that the BSA surface has only a limited number of binding sites/surface for the dendrimer, this result also suggests that dendrimers also bind to the PEG attached to the protein. The binding mechanism of PEG to dendrimer cations may be due to PEG's ability to bind cations, such as K^+ or Na^+ [38]. We can speculate that the charge of BSA (-18 at pH 7.4 in PBS buffer) is compensated by dendrimer bound to the surface and repels dendrimer bound to PEG, leading to a more extended configuration of PEG around the protein. On the other hand, surface bound dendrimers might also bind PEG at a free dendrimer surface, leading to an increased protection of the protein and PEG configurations closer to the protein surface. It is important to note here the molecular weight of the PEG relative to dendrimer size. For 5k PEG, it might be difficult to interact with more than one dendrimer with a molecular weight of ~3.6k (even if their conformations are quite different). 20k-PEG might wrap one or more dendrimers bound to the protein surface or bind to dendrimers that are unattached to the protein surface.

3.4 Protective role of PEGylation in presence of dendrimers

PEGylation is used to increase bioavailability and protect proteins from digestion. To check whether dendrimer addition and any special dendrimer PEG interaction alters protection from proteolysis, we used trypsin that cuts BSA into a larger 50kDa and a smaller 12kDa fragment.

BSA, 5k-PEG-BSA and 20k-PEG-BSA were tested under 3 different conditions: alone, with added dendrimer in a 1:4 molar ratio, and adding dendrimers in a 1:4 molar ratio and trypsin. The protein solution was examined by SDS-PAGE using microfluidics-based electrophoresis with a Bioanalyzer Agilent 2100. Figure 5A shows that after trypsin digestion 2 new peaks appear at 12 kDa and 50 kDa as BSA fragments. This indicates that dendrimers do not protect BSA against trypsin digestion. For 5k-PEG BSA, there were no fragments, indicating good protection from digestion. In the case of 20k-PEG BSA, a minor peak at ~50k was seen that might be due to a small fraction of non-PEGylated BSA. Apart from this, we found protection from trypsin digestion.

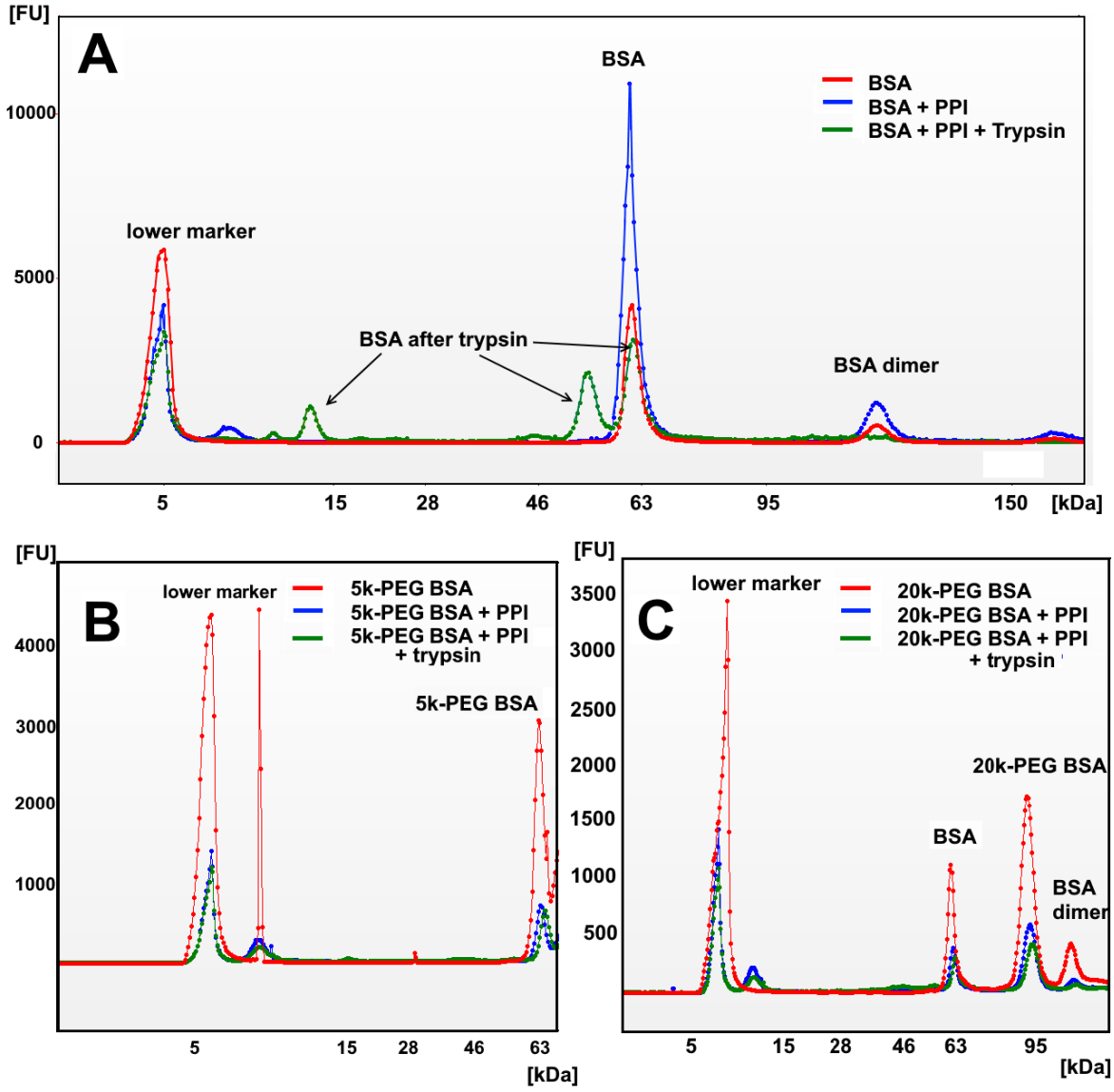

Figure 5. *Bioanalyzer spectra obtained from SDS-PAGE microfluid-based electrophoresis. Main peaks relate lower marker (5kDa, reference), BSA (65kDa) and BSA dimer (130kDa). The peak at 8kDa comes from dye- labelled gel. PEGylated BSA shows a shift relative to BSA with respect to the added PEG chain. For 20k-PEG BSA, a fraction of unlabelled BSA is seen. The charged dendrimers seem to interact with the lower marker and the dye used for labelling, making direct comparison of intensities difficult.*

3.5 Microscopic view of PEGylated BSA with dendrimers.

The effect of dendrimers and their complexes with unPEGylated and PEGylated albumin was examined by TEM after drying the complex solution. Figure 6 A shows only the dendrimer morphology. The images in Figure 6 B and C indicate the ability of dendrimers to create complexes with BSA. The aggregate size of PPI alone varied from 50 to 200 nm. The images show changes in shape and morphology of the complexes. The size of the complexes in both cases was very large (>1,000 nm) showing that the complexes of dendrimer and BSA have a high tendency to aggregate. However, it is noteworthy that the complex of PEGylated BSA (20kDa PEG) and dendrimers looks more coarse-grained compared to the complex of non-PEGylated albumin. Assuming an attractive interaction between PEG and the dendrimers, this might bring aggregates closer together bridging the gap between BSA during the drying process, resulting in more homogenous and denser aggregates (Figure 6 C).

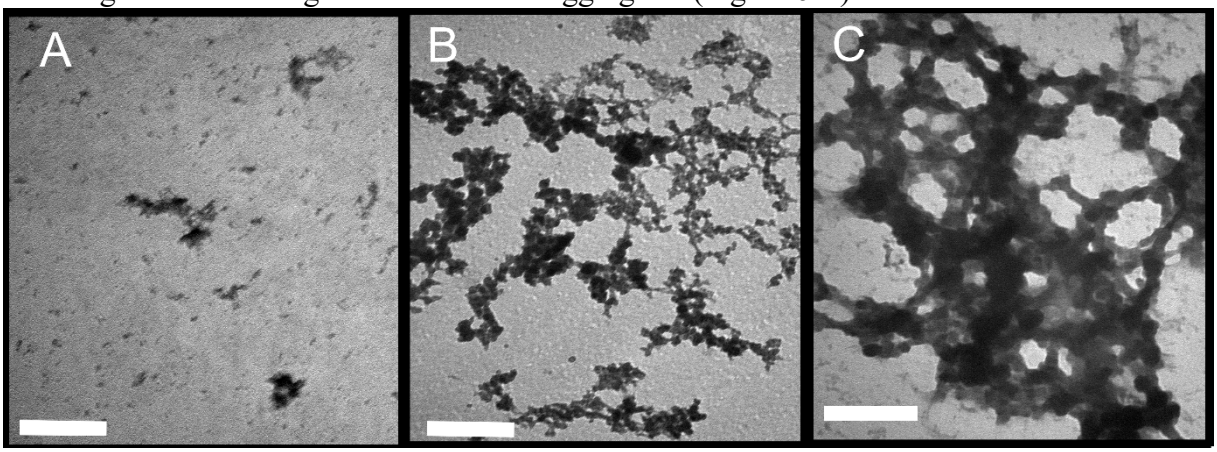

Figure 6*. Electron micrographs of PPI dendrimers (A) and dendrimer/protein mixtures composed of PPI dendrimers and BSA (B) and PPI dendrimers and 20k-PEG-BSA (C). The molar ratio (protein:dendrimers) of complexes was 1:4; bar =200 nm.*

4. Conclusions

The interaction of dendrimers with PEGylated BSA shows a significant change compared to BSA that suggests a strong additional interaction of dendrimers with PEG that leads to binding of PEG to dendrimers. A major indication is found in the increased forward scattering of SAXS, showing more than only additive contributions in the forward scattering. The change in morphology of dried PEGylated BSA with dendrimers also supports the binding of dendrimers to PEG. An important observation is the small decrease in fluorescence quenching for 5k-PEG compared to the nearly complete quenching of Trp134. Since there was no change in the CD spectroscopy and the high Q pattern in SAXS, we can exclude that possibility that changes of the secondary structure or of the domain structure are responsible for the effects on fluorescence quenching. The negligible quenching for 5k-PEG indicates a preferential binding of the dendrimers to PEG, leaving the Trp134 environment relatively unchanged. For 20k-PEG binding of several dendrimers to PEG and protein could induce a collapse of the PEG chain onto the protein surface, leading to almost complete suppression of fluorescence. Collapse of the PEG chain depends strongly on the molecular weight and salt concentration [39]. PEG aggregates are still highly hydrated, presenting a hydrophilic environment to the Trp134 [40].
We have focused on the mechanism of interaction between PEGylated albumin and polypropylene imine dendrimers G4. The results clearly show that cationic dendrimers bind to PEG and/or the protein surface. Exploiting the collapse of the PEG dendrimer complex on BSA as a protective mechanism it might be possible to enhance dendrimer transport in the body (Figure 7).

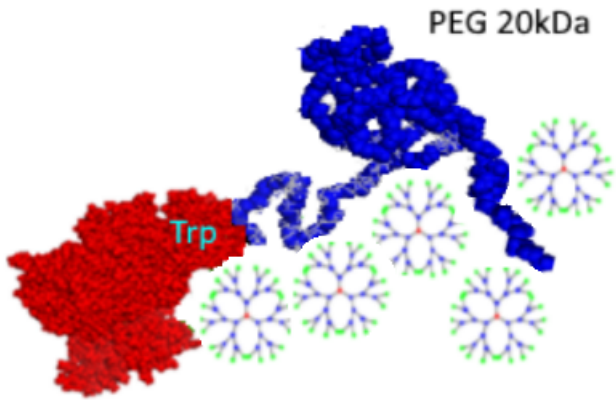

Figure 7. *Possible mechanism of interaction between dendrimers and PEGylated BSA.*

Acknowledgements

We thank Dr. Wojciech Trybus from the Department of Cell Biology at the Jan Kochanowski University, Kielce, Poland, for his help in obtaining TEM microscopy pictures.

Conflict of Interest

There is no conflict of interest.

References

(1) Contin, M.; Garcia, C.; Dobrecky, C.; Lucangioli, S.; D'Accorso, N. Future Med. Chem. **2019**, *11* (14), 1791–1810.

(2) Michlewska, S.; Ionov, M.; Maroto-Díaz, M.; Szwed, A.; Ihnatsyeu-Kachan, A.; Loznikova, S.; Shcharbin, D.; Maly, M.; Ramirez, R. G.; de la Mata, F. J.; Bryszewska, J. Inorg. Biochem. **2018**, *181,* 18-27

(3) Ionov, M.; Ciepluch, K.; Klajnert, B.; Glinska, S.; Gomez-Ramirez, R.; Javier, F.; Mata, D.; Munoz-Fernandez, M. A.; Bryszewska, M. Colloids and Surfaces B : Biointerfaces. **2013**, *101*, 236–242.

(4) Wu, L.; Ficker, M.; Christensen, J. B.; Trohopoulos, P. N.; Moghimi, S. M. Bioconjug Chem. **2015**, *26*, 1198-211

(5) Mignani, S. M.; Brahmi, N. El; Kazzouli, S. El; Laurent, R.; Ladeira, S.; Caminade, A.;

Pedziwiatr-werbicka, E.; Szewcyk, E. M.; Bousmina, M. M.; Cresteil, T.; Majoral, J. P. Mol. Pharmaceutics, 2**017**, *14*, 4087-4097.

(6) Ziemba, B.; Franiak-Pietryga, I.; Pion, M.; Appelhans, D.; Munoz-Fernandez, M. Á.; Voit, B.; Bryszewska, M.; Klajnert-Maculewicz, B. Int J Pharm. **2014**, *461*, 391–402.

(7) Janaszewska, A.; Lazniewska, J.; Trzepiński, P.; Marcinkowska, M.; Klajnert-Maculewicz, B. Biomolecules **2019**, *9* , 1-23.

(8) Pedziwiatr-Werbicka, E.; Milowska, K.; Dzmitruk, V.; Ionov, M.; Shcharbin, D.; Bryszewska, M. Eur. Polym. J. **2019**, *119*, 61–73.

(9) Ciepluch, K.; Nyström, B.; Appelhans, D.; Zablocka, M.; Bryszewska, M.; Majoral, J. P. J. Polym. Res. **2015**, *22,* 9.

(10) Szulc, A.; Pulaski, L.; Appelhans, D.; Voit, B.; Klajnert-Maculewicz, B. Int. J. Pharm. **2016**, *513*, 572–583.

(11) Jatczak-Pawlik, I.; Gorzkiewicz, M.; Studzian, M.; Appelhans, D. Voit, B.; Pulaski, L.; Klajnert-Maculewicz, B. Pharm. Res. **2017**, *34*, 136–147.

(12) Yamashita, S.; Katsumi, H.; Hibino, N.; Isobe, Y.; Yagi, Y.; Kusamori, K.; Sakane, T.; Yamamoto, A. J. Control. Release. **2017**, *262*, 10-17

(13) Mandeville, J. S.; Tajmir-Riahi H. A. Biomacromolecules, **2010**, *11*, 465–472.

(14) Sekowski, S.; Buczkowski, A.; Palecz, B.; Gabryelak, T. Spectrochim. Acta Part A Mol. Biomol. Spectrosc. **2011**, *81* , 706–710.

(15) Klajnert, B.; Appelhans, D.; Komber, H.; Morgner, N.; Schwarz, S.; Richter, S.; Brutschy, B.; Ionov, M.; Tonkikh, A. K.; Bryszewska, M.; Voit, B. Chemistry, **2008**,*14*, 7030–7041.

(16) Aravinthan, A.; Kamala-Kannan, S.; Govarthanan, M.; Kim, J. H. Toxicol. Res. (Camb). **2016**, *5*, 1530–1538.

(17) Kratz, F. J. Control. Release **2008**, *132*, 171–183.

(18) Dadparvar, M.; Wagner, S.; Wien, S.; Kufleitner, J.; Worek, F.; Briesen, H. Von;

Kreuter, J. Toxicol. Lett. **2011**, *206*, 60–66.

(19) Elsadek, B.; Kratz, F. J. Control. Release **2012**, *157*, 4–28.

(20) Larsen, M. T.; Kuhlmann, M.; Hvam, M. L.; Howard, K. A. Mol. Cell. Ther. **2016**, 1–12.

(21) Zhao, M.; Li, H.; Bu, X.; Lei, C.; Fang, Q.; Hu, Z. ACS Nano **2015**, *9*, 10099–10112.

(22) Lee, P.; Wu, X. Curr Pharm Des **2015**, *21*, 1862–1865.

(23) Sleep, D.; Cameron, J.; Evans, L. R. BBA - Gen. Subj. **2013**, 1–9.

(24) Zhang, S.; Kucharski, C.; Doschak, M. R.; Sebald, W.; Uludağ, H. Biomaterials **2010**, *31*, 952–963.

(25) Azizi, M.; Ghourchia, H.; Yazdian, F.; Bagherifam, S.; Bekhradnia, S.; Nyström B. Sci Rep. **2017**, *7*, 1–18.

(26) Azizi, M.; Ghourchian, H.; Yazdian, F.; Alizadehzeinabad H. Artif. Cells, Nanomedicine, Biotechnol. **2018**, *0*, 1–11.

(27) Reddy, K. R.; Modi, M. W.; Pedder, S. Adv Drug Deliv Rev. **2002**, *54*, 571–586.

(28) Albani, J. R. J Fluoresc. **2014**, *24*, 93–104.

(29) Shcharbin, D.; Janicka, M.; Wasiak, M.; Palecz, B.; Przybyszewska, M.; Zaborski, M.; Bryszewska, M. **2007**, *1774*, 946–951.

(30) Smeijers, A. F.; Markvoort, A. J.; Pieterse, K.; Hilbers, P. A. J. J. Chem. Phys. **2016**, *144*.

(31) Rietveld, I. B.; Smit, J. A. M. Macromolecules **1999**, *32*, 4608–4614.

(32) Wu, J.; Zhao, C.; Lin, W.; Hu, R.; Wang, Q.; Chen, H.; Li, L.; Chen, S.; Zheng, J. *J.* Mater. Chem. B **2014**, *20*, 2983.

(33) Israelachvili, J. Proc. Natl. Acad. Sci. U. S. A. **1997**, *94*, 8378–8379.

(34) Froehlich, E.; Mandeville, J. S.; Jennings, C. J.; Sedaghat-Herati, R.; Tajmir-Riahi H.A. J Phys Chem B. **2009**, *113*, 6986–6993.

(35) Wrobel, D.; Marcinkowska, M.; Janaszewska, A.; Appelhans, D.; Voit, B.; Klajnert-

Maculewicz, B.; Bryszewska, M.; Stofik, M.; Herma, R.; Duchnowicz, P.; Maly, J. Colloids and Surfaces B : Biointerfaces. **2017**, *152*, 18–28.

(36) Ferebee, R.; Hakem, I. F.; Koch, A.; Chen, M.; Wu, Y.; Loh, D.; Wilson, D. C.; Poole, J. L.; Walker, J. P.; Fytas, G.; Bockstaller, M. R. J. Phys. Chem. B **2016**, *120*, 4591–4599.

(37) Ciepluch, K.; Radulescu, A.; Hoffmann, I.; Raba, A.; Allgaier, J.; Richter, D.; Biehl, R. Bioconjug. Chem. **2018**, *29*, 1950–1960.

(38) Breton, M. F.; Discala, F.; Bacri, L.; Foster, D.; Pelta, J.; Oukhaled, A. J. Phys. Chem. Lett. **2013**, *4*, 2202–2208.

(39) Bailey, F. .; Callard, R. W. Appl. Polym. Sci. **1959**, *1*, 56–62.

(40) Thiyagarajan, P.; Chaiko, D. J.; Hjelm, R. P. Macromolecules **1995**, *28*, 7730–7736.

GRAPHICAL CONTENTS ENTRY

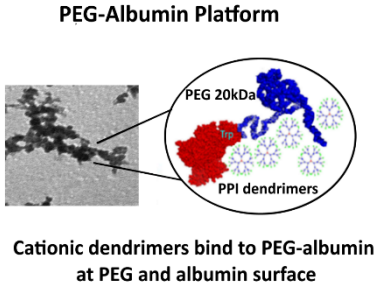

Figure legends

Figure 1. Structure of bovine serum albumin with three different domains. Cys34 (place where PEG is attached) and Trp134 are localized on the same domain (A). The chemical structure of polypropylene(imine) dendrimers with amine terminated groups on the surface and a molecular weight of about 3600 Da (B). G4 PPI dendrimers have a Rg of about 1.2 nm and geometrical radius of about 1.3 nm [30,31].

Figure 2. BSA, 5kPEG-BSA and 20kPEG-BSA tryptophan residue fluorescence quenching by poly(propylene imine) dendrimers. The molar ratio of proteins : dendrimers was 1:4. Values are given relative to BSA taken as 100%.

Figure 3. CD spectra of BSA, 5k-PEG-BSA and 20k-PEG-BSA mixed with poly(propylene imine) dendrimers – PPI.

Figure 4. SAXS form factors as extracted from concentration series measurements for BSA, 5k-PEG-BSA and 20PEG-BSA with and without PPI dendrimers. The BSA characteristic linear region between 1-2.5 nm-1 for all samples indicated preservation of protein structure. Changes were observed mainly between 0.2 and 1.2 nm-1 and represent a change in the radius of gyration due to dendrimers and PEG. Data are scaled by a factor of 10 for better visibility.

Figure 5. Bioanalyzer spectra obtained from SDS-PAGE microfluid-based electrophoresis. Main peaks relate lower marker (5kDa, reference), BSA (65kDa) and BSA dimer (130kDa). The peak at 8kDa comes from dye- labelled gel. PEGylated BSA shows a shift relative to BSA with respect to the added PEG chain. For 20k-PEG BSA, a fraction of unlabelled BSA is seen. The charged dendrimers seem to interact with the lower marker and the dye used for labelling, making direct comparison of intensities difficult.

Figure 6. Electron micrographs of PPI dendrimers (A) and dendrimer/protein mixtures composed of PPI dendrimers and BSA (B) and PPI dendrimers and 20k-PEG-BSA (C). The molar ratio (protein:dendrimers) of complexes was 1:4; bar =200 nm.

Figure 7. Possible mechanism of interaction between dendrimers and PEGylated BSA.